Supplementary Information (SI) for Journal of Materials Chemistry A.
This journal is © The Royal Society of Chemistry 2025

Electronic Supporting Information

for

A Colorimetric Ammonia Sensor Based on an Interfacial Porous Polymer Membrane: Coupled Hydrogen-Bonding and Electronic Structure Modulation

Zebiao Qiu, ‡ Qianchi Xiong, ‡ Heng Zhang, Yue Xiao, Ling Zhang, Ruijuan Wen, Liping Ding*, Haonan Peng* and Yu Fang

Key Laboratory of Applied Surface and Colloid Chemistry (Ministry of Education), Shaanxi Key Laboratory of New Conceptual Sensors and Molecular Materials, School of Chemistry and Chemical Engineering, Shaanxi Normal University, Xi’ an 710062, P. R. China

* Corresponding author: dinglp33@snnu.edu.cn, phn@snnu.edu.cn

Contents

1. Reagents and Materials

2. Experimental Details

3. Instrumental methods

4. Supplementary Table and Figures

5. Supplementary Reference

1. Reagents and Materials

2,6-Diformylphenol and 5-Hydroxyisophthalaldehyde in 98% purity were obtained from Bidepharm. Benzene-1,3,5-tricarbohydrazide at 98% purity was obtained from Adamas-beta. acetic acid was obtained from Merck (>99.5%), and the water used was supplied by Milli-Q water (Milli-Q EQ 7000, Merck). All the solvents used in the study were purchased from China National Medicines Corporation Ltd. and used without further purification unless otherwise stated.

2. Experimental Details

2.1 Fabrication of the BTH-DFP membrane

First, 4 mL of DFP (0.64 mg) was prepared in DCM solution. Then, 0.57 mg of BTH was weighed and dissolved in DMSO/H_2O solution (4mL with the Ratio of 1:1). The DCM solution was transferred to take 10 mL of specimen petri dish, subsequently, 1 mL of acetic acid was added, and then the configured DMSO/H_2O solution was slowly added to the upper layer of DCM. The DCM/H_2O interface was formed. The dish was left at room temperature in an undisturbed get state for 3-4 days. The membrane BTH-DFP was generated at the DCM/H_2O interface. Removal of the top H_2O layer using a rubber-tipped burette. The membrane was then transferred to filter paper and was washed with ethanol with dichloromethane. Pure membranes were obtained.

2.2 The calculation of ΔRGB

The total color difference (ΔRGB) was calculated from the RGB values extracted from the membrane images before and after NH3 exposure using the following formula:

$$\Delta RGB = (R_a + G_a + B_a) - (R_b + G_b + B_b)$$

Where *Ra, Ga, Ba* represent the red, green, and blue values after NH_3 exposure, and *Rb, Gb, Bb* represent the corresponding values before exposure.

2.3 Preparation of Analyte Vapors.

For Vapor phase sensing of liquid analytes, the analyte to be tested (example: ammonia) is prepared as described below: 50 mL of ammonia is placed in a 500 mL brown bottle, sealed, and placed under test conditions for 24 h. The system reaches gas-liquid equilibrium, at which point the gas inside the bottle can be considered to be the saturated vapor of ammonia. ammonia vapor can be mixed with dry air using a syringe to obtain different concentrations of ammonia vapor, which is injected into a gas bag for subsequent testing.

2.4 Sensing test conditions

Temperature: 24 – 25 °C, consistently maintained throughout the experiment. Humidity: ranging from 40% to 45%.

3. Instrumental methods

The chemical composition of the membrane was characterized by Fourier transform infrared spectroscopy (TENSOR27, Bruker) and X-ray photoelectron spectroscopy (XPS, AXIS ULTRA). The morphology of the membrane was characterized by scanning electron microscopy (SEM, SU8220), high resolution transmission electron microscopy (HR-TEM, JEM-2100) and atomic force microscopy (AFM, Dimension ICON). The contact angle of the nanomembrane was measured using a contact angle meter (OCA20, Dataphysics). XRD analysis was performed using a Cu Kα irradiation source (λ = 1.5418 Å, Bruker D8 Discover) x-ray diffractometer. The UV-Vis absorption spectra of the membrane were collected using a U-3900 spectrophotometer (Hitachi). The sensing properties of the membrane were determined by a laboratory-made sensing platform. The optical images presented in this study were taken with a Nikon Z30 camera.

4. Supplementary Table and Figures

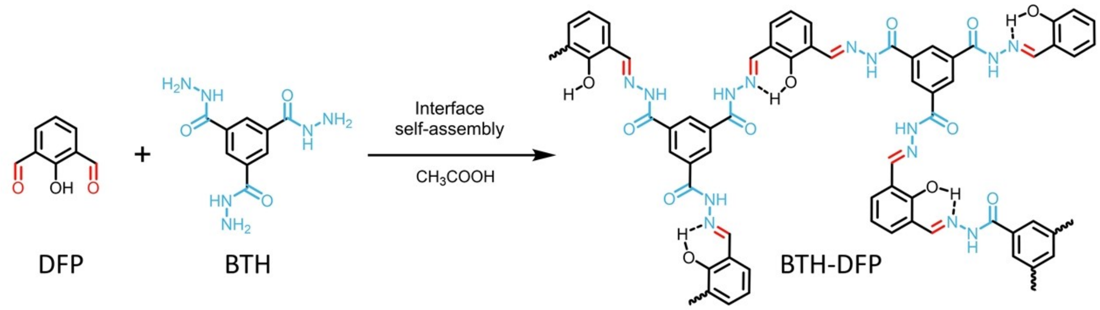

Figure S1. Synthesis route of BTH-DFP membrane.

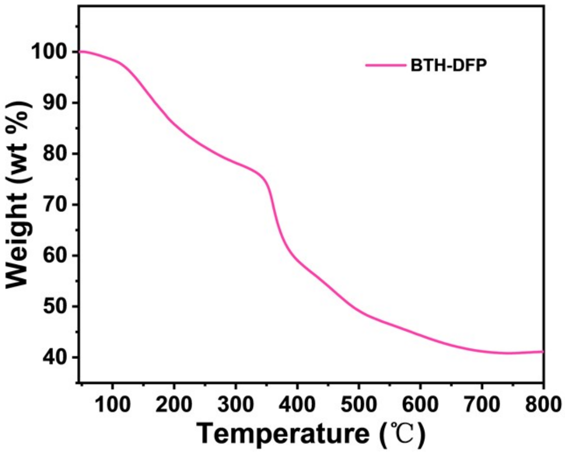

Figure S2. TGA curve of the BTH-DFP membrane.

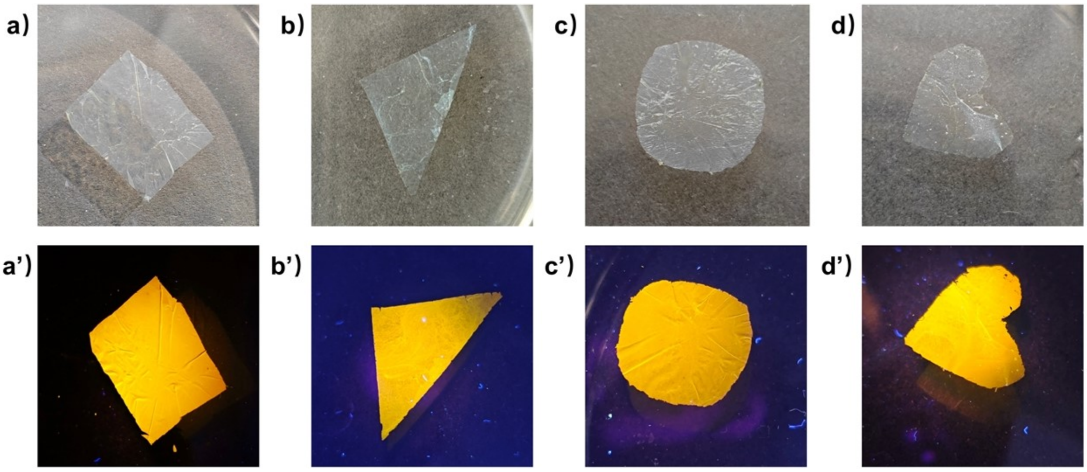

Figure S3. Photographs of the BTH-DFP membrane processed into various shapes—(a) rectangle, (b) triangle, (c) circle, and (d) heart—under ambient daylight (a–d) and UV illumination at 365 nm (a' - d').

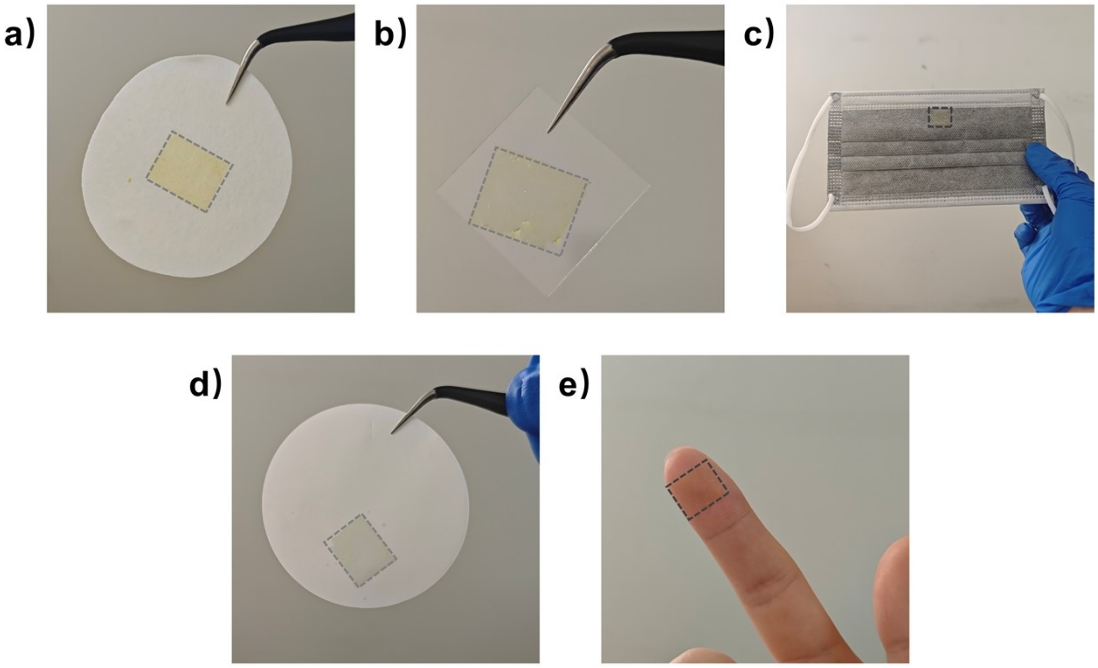

Figure S4. Photographs demonstrating the strong adhesion of the BTH-DFP membrane to various substrates, including (a) filter paper, (b) glass, (c) face mask, (d) PET film, and (e) human skin.

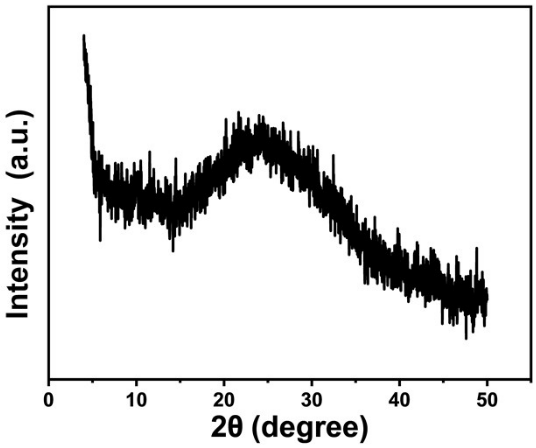

Figure S5. XRD spectra of BTH-DFP membrane.

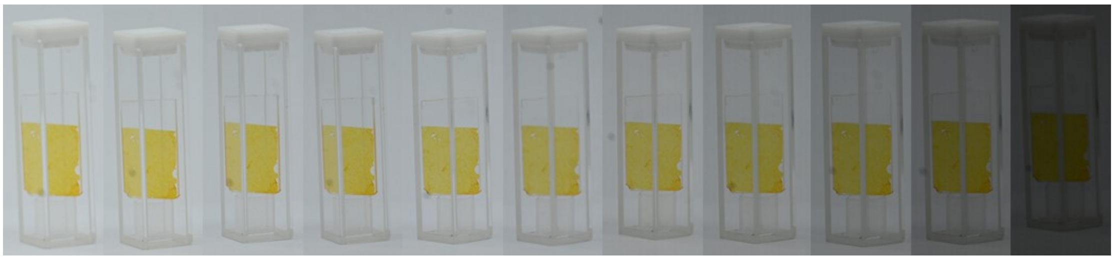

Figure S6. Photographs of the membrane sensor exposed to NH_3 under different lighting intensities.

Note: A series of photographs captured under different lighting conditions demonstrate that the NH_3-induced color change remains clearly discernible across a range of illumination levels. These results indicate that the sensor's performance is not limited to daylight conditions.

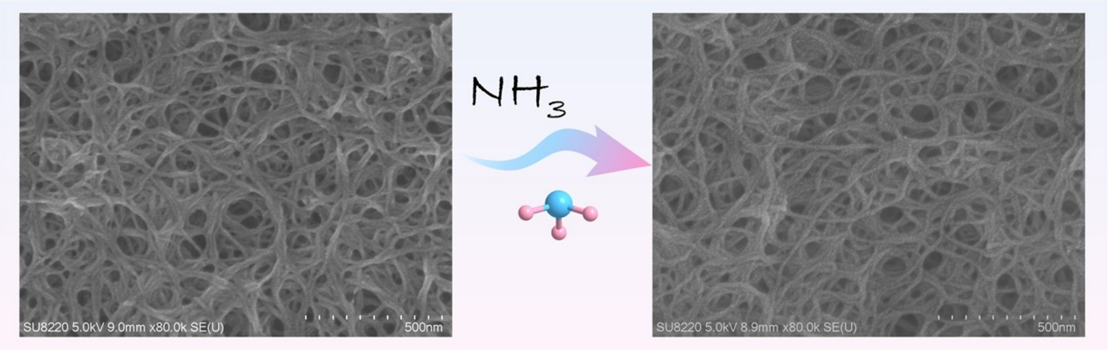

Figure S7. SEM images of BTH-DFP membrane before and after exposure to NH_3.

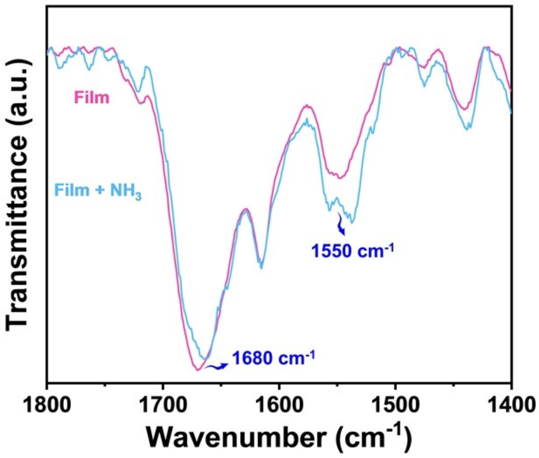

Figure S8. FTIR spectra before and after NH_3 exposure in the 1400-1800 cm^{-1} region.

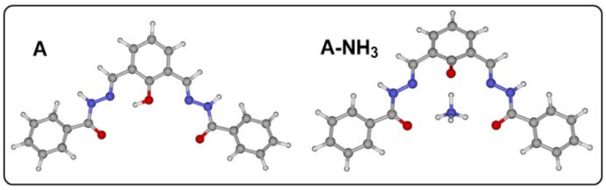

Figure S9. Top-view structures of model compound A before and after NH$_3$ adsorption.

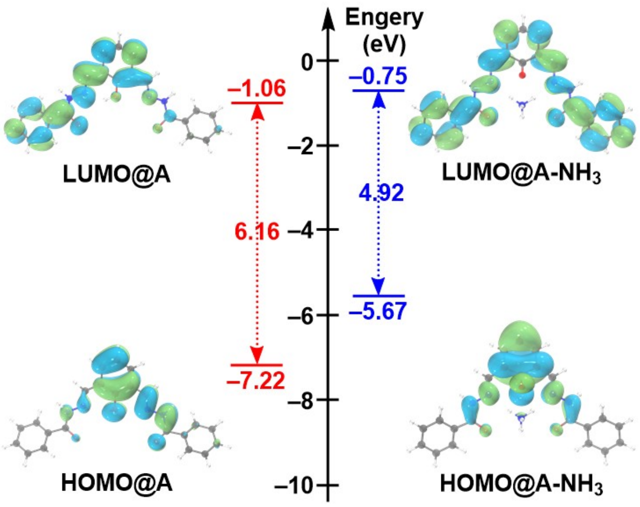

Figure S10. The frontier molecular orbital (HOMO/LUMO) of model compound A and A-NH_3.

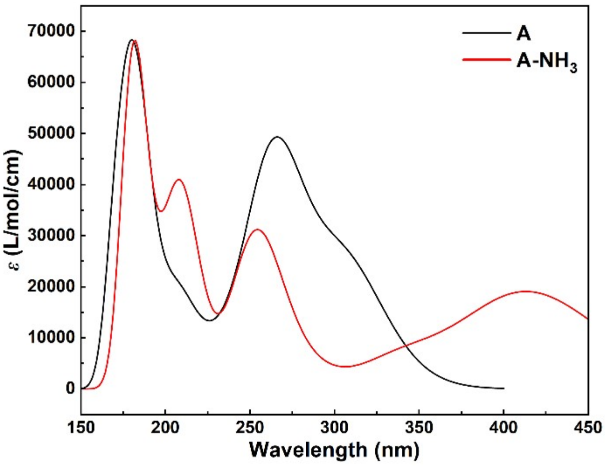

Figure S11. Simulated UV–vis absorption spectra of model compound A and A-NH_3

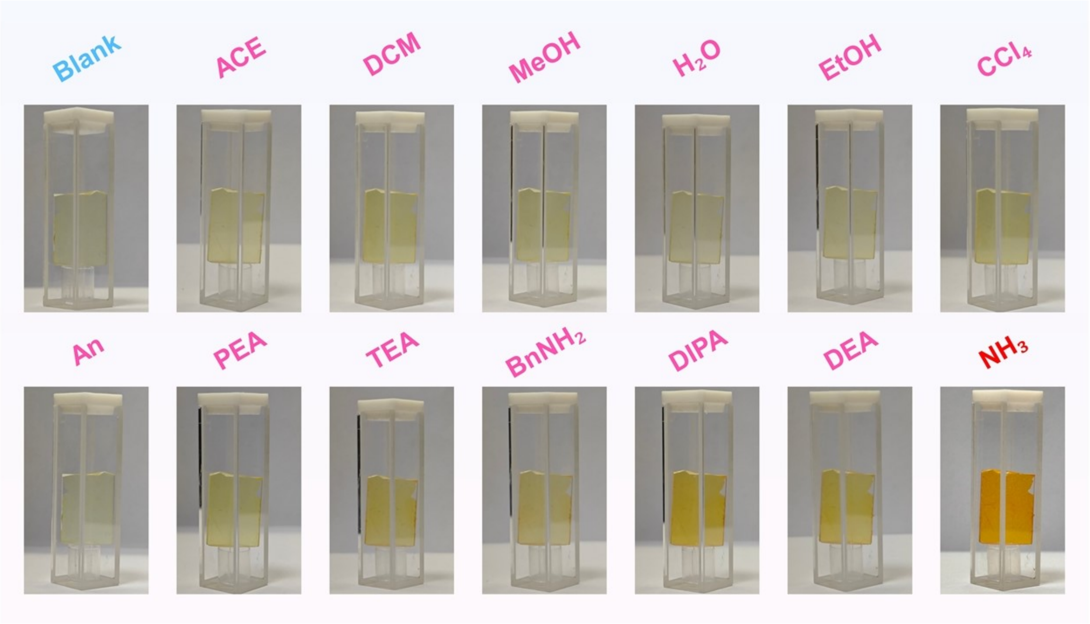

Figure S12. Photograph of the BTH-DFP membrane after exposure to various volatile organic compounds (VOCs).

Note: ACE - Acetone, DCM - Dichloromethane, MeOH - Methanol, H_2O - Water, EtOH - Ethanol, CCl_4 - Carbon tetrachloride, An - Aniline, PEA - Phenylethylamine, TEA - Triethylamine, $BnNH_2$ - Benzylamine, DIPA - Diisopropylamine, DEA - Diethylamine, NH_3 - Ammonia.

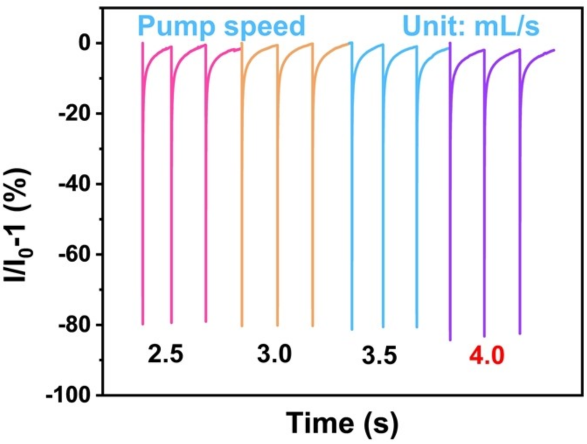

Figure S13. Optimization of pump speed for the BTH-DFP membrane.

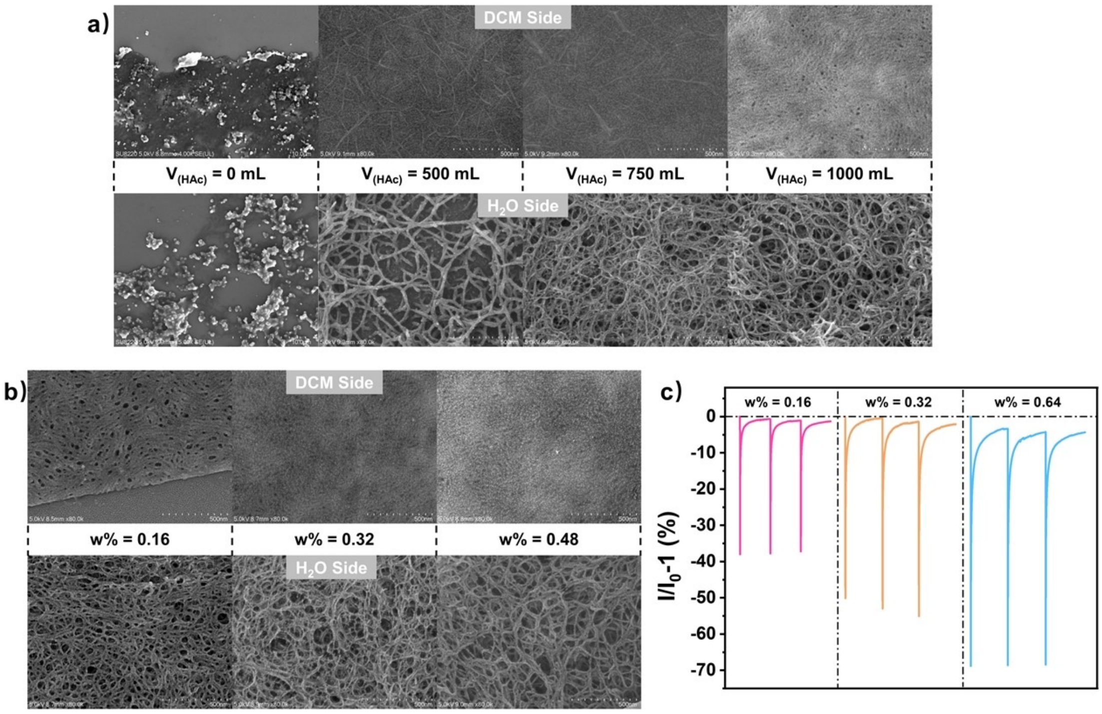

Figure S14. (a) SEM images of membranes prepared with varying concentrations of HAc. (b) SEM images of membranes prepared with varying concentrations of precursor solutions. (c) NH_3 sensing performance of laminated sensors using membranes with different pore structures.

Note: The masses of monomers DFP and BTH were adjusted proportionally throughout the system. The concentration of the system was defined as the mass-to-volume ratio of DFP to the solvent DCM.

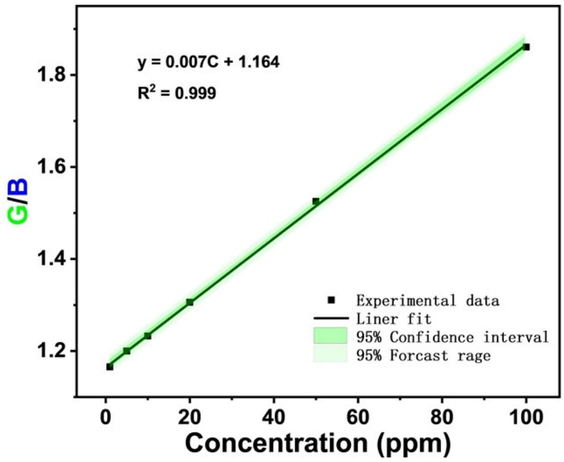

Figure S15. Linear relationship between G/B ratio and NH_3 concentration (0-100 ppm).

Table S1. Comparison of NH_3 sensing between this work and other methods.

Materials	**Sample**	**Detection technique**	**Detection Limit**	**Response time**	**References**
BTH-DFP	Gas	Colorimetric + Laminated Sensor	1ppm	1s	This work
P4TI	Gas	morphology effect	1-100 ppm	1-3 min	1
$Ti_3C_2T_X$ MXene@TiO_2/ MoS_2	Gas	Chemiresistive	500 ppb	117 s	2
PA6/PANI	Gas	Chemiresistive	10 ppb	171 s	3
TPCH-mOBPy COF	Gas	Fluorescent Sensor	51.8 ppm	0.65 s	4
Co_3O_4-$CoFe_2O_4$	Gas	Chemiresistive	100 ppm	15 s	5
C-600	Gas	Chemiresistive	0.1 ppm	37.5 s	6
PrO_X/In_2O_3/ WO_3 (PIW)	Gas	Chemiresistive	0.5 ppm	7 s	7
Au/HT-Nb_2CT_x	Gas	Chemiresistive	0.5 ppm	14 s	8
$CuCO_2O_4$	Gas	Chemiresistive	100 ppm	50 s	9
PPM10	Gas	Chemiresistive	500 ppb	92 s	10
PDI-PF	Gas	Charge transfer	200 ppb	104 s	11
BFCUR-ENF	Gas	Fluorescent Sensor	22 ppb	80 ms	12
PFOTES-CNF	Gas	electron transfer	10 ppm	12 s	13
SnS_2	Gas	Chemiresistive	20 ppb	250 s	14

5. Supplementary Reference

1. C. F. Lu, C. W. Shih, C. A. Chen, A. Chin and W. F. Su, *Adv. Funct. Mater.*, 2018, **28**, 1803145.
2. X. Tian, L. Yao, X. Cui, R. Zhao, T. Chen, X. Xiao and Y. Wang, *J. Mater. Chem. A*, 2022, **10**, 5505-5519.
3. Y. Zhou, Y. Zhang, Y. Zhou, L. Zhao, F. Liu, X. Yan, P. Sun and G. Lu, *Nano Energy*, 2023, **117**, 108881.
4. J. Li, Y. Wan, G. Jiang, Y. Ozaki and F. Pi, *Chem. Eng. J.*, 2024, **479**, 147746.
5. J. Hu, X. Xiong, W. Guan, Y. Chen and H. Long, *Chem. Eng. J.*, 2023, **452**, 139346.
6. H. Zhu, H. Ji, Z. Yuan, Y. Shen, H. Gao and F. Meng, *J. Mater. Chem. A*, 2023, **11**, 10565-10576.
7. W. Gao, X. Chang, O. Ola, Z. Wang, Q. Liao, X. Zhu, J. Li, Y. Jiang, D. Wang and S. Sun, *Chem. Eng. J.*, 2025, **509**, 161482.
8. T. Zhou, P. Zhang, Z. Yu, M. Tao, D. Zhou, B. Yang and T. Zhang, *Nano Energy*, 2023, **108**, 108216.
9. K. K. Pawar, A. Mirzaei, S. Sub Kim and H. W. Kim, *Chem. Eng. J.*, 2024, **482**, 148890.
10. C. Chen, Q. Tu, X. Zhou, J. Xu, C. Lv, X. Ke, H. Li, L. Chen and X. Liu, *Adv. Compos. Hybrid Mater.*, 2024, **8**, 98.
11. B. M. Oh, S. H. Park, J. H. Lee, J. C. Kim, J. B. Lee, H. J. Eun, Y. S. Lee, B. E. Seo, W. Yoon, J. E. Kwon, H. Yun, S. K. Kwak, O. P. Kwon and J. H. Kim, *Adv. Funct. Mater.*, 2021, **31**, 2101981.
12. G. Song, D. Jiang, J. Wu, X. Sun, M. Deng, L. Wang, C. Hao, J. Shi, H. Liu, Y. Tian and M. Chen, *Chem. Eng. J.*, 2022, **440**, 135979.
13. W. Zhang, J. Zhao, C. Cai, Y. Qin, X. Meng, Y. Liu and S. Nie, *Adv. Sci.*, 2022, **9**, e2203428.
14. H. Chen, Y. Chen, H. Zhang, D. W. Zhang, P. Zhou and J. Huang, *Adv. Funct. Mater.*, 2018, **28**. 1801035